

Robust Signal Reconstruction Using the Prolate Spherical Wave Functions and Maximum Correntropy Criterion [†]

Cuiming Zou* and Kit Ian Kou[†]

Department of Mathematics, Faculty of Science and Technology, University of Macau,
Macao, China

Abstract

Signal Reconstruction is one of the most important problem in signal processing. This paper proposes a novel signal reconstruction method based on the prolate spherical wave functions (PSWFs) and maximum correntropy criterion (MCC). The PSWFs are a kind of special functions, which have been proved having good performance in signal reconstruction. However, the existing PSWFs based reconstruction methods only consider the mean square error (MSE) criterion as the cost functions. The MSE criterion is sensitive to the non-Gaussian noise, since it is builded up by the Gaussian assumption. Therefore, for the impulsive noise or outliers, the MSE based reconstruction methods will lead to the large reconstruction error. The proposed MCC and PSWFs based robust signal reconstruction method can reduce the impact of large and non-Gaussian noise. The experimental results on the synthetic signals show that the proposed method can improve the MSE with notable gains in most cases.

Keywords: Signal reconstruction; prolate spherical wave functions; Gaussian noise

1 Introduction

Prolate spheroidal wave functions (PSWFs) are important functions in information and communication theory [1]. They, which is a special case of the spheroidal wave functions, possess many interesting properties, such as double orthogonality in both the finite time domain and the

*zoucuiming2006@163.com

[†]Corresponding author: kikou@umac.mo

whole real axis. The PSWFs are the most energy concentrated signals in energy concentration problem which was studied by Slepian *et al.* [2, 3, 4]. In practical, their discrete forms also satisfy the orthogonality relations. The energy concentration problem aims to find the bandlimited functions with the maximum energy in a fixed time interval, which satisfies the extreme conditions in the uncertainty principle [5]. The PSWFs are proved to be an orthogonal basis in the Paley-Wiener space [1, 6], which has extensively used for a variety of physical and engineering applications.

Most notably, the PSWFs have been used successfully in sampling theory and signal reconstruction. The famous Shannon's sampling theorem was created in 1949 [7], which is the foundation of information theory. The reconstruction formula is $f(x) = \sum_{k \in \mathbb{Z}} f(kW) \text{Sinc}\left(\frac{x}{W} - k\right)$, which is known as the cardinal series expansion (basis functions obtained by appropriate shifting and rescaling of the sinc-functions). Nowadays this theorem still plays a central role in signal, image processing and communication. In [8, 9], researchers studied some Shannon's reconstruction formulas associated with PSWFs. The sinc-function Sinc was introduced by the expansions of PSWFs' (also namely Slepian series) [10, 11].

In 2009, Senay *et al.* [12] first utilized the PSWFs to the signal reconstruction problem. They later extended the reconstruction method combining with the Tikhonov regularization in [13]. However, most existing signal reconstruction methods exploit the mean square error (MSE) criterion as the cost functions due to the ease of analysis. It is well known that the MSE is build by the hypothesis that the noise follows the Gaussian distribution. In reality, the noises are more complicated and do not necessarily obey the Gaussianity assumption, for example the impulsive noise [14]. Once the assumption violates, the performance of the MSE based reconstruction methods may severely decline. In this paper, we propose a novel signal reconstruction method which is based on the maximum correntropy criterion (MCC) in the information-theoretic learning [15, 16]. Unlike the MSE, the MCC is independent of the noise distribution. This makes our method more attractive in handling both Gaussian and non-Gaussian noise cases.

The paper is organized as follows. Section 2 introduces some basic facts about PSWFs and maximum correntropy criterion. Section 3 recalls the classical sampling theorem and relationship of sinc-functions and PSWFs. We discuss the existing PSWFs based reconstruction methods and our proposed methods. Section 4 presents the experimental results for uniformly sampling signal and non-uniformly sampling signal. For both of the experiments, our proposed methods show good performances compare to the other related methods. Some conclusions are drawn, and future works are proposed in Section 5.

2 Preliminaries

The present section collects some basic facts about PSWFs and the maximum correntropy criterion. We first introduce some mathematical notations throughout the paper. Vectors will be denoted as the boldface lowercase letters, i.e., \mathbf{x} . Matrices will be denoted by the boldface

uppercase letters, i.e., \mathbf{A} . The i -th component of \mathbf{x} is x_i and the i, j element of \mathbf{A} is $(\mathbf{A})_{ij}$.

2.1 Prolate Spherical Wave Functions

Finding the most energy concentrated signals both in fixed time and frequency domains at the same time is a fundamental problem in information theory [2, 6, 17]. The problem was studied by Slepian et al. in the early's 1960 [2, 18, 19], and the solutions are the prolate spherical wave functions (PSWFs). In this part, we review the basic facts about this functions in continuous and discrete cases.

2.1.1 Continuous Case:

The continuous PSWFs $\{\varphi_n\}_{n=0}^{\infty}$ are solutions of the integral equation

$$\int_{-\tau}^{\tau} \varphi_n(s) \frac{\sin \sigma(t-s)}{\pi(t-s)} ds = \alpha_n \varphi_n(t), \quad (2.1)$$

where $[-\tau, \tau]$ and $[-\sigma, \sigma]$ are the fixed time and frequency domains, respectively. The continuous PSWFs have several interesting properties, which follow from the general theory of integral equations and the work by Slepian *et al.* [1, 20, 21, 22]. We list some of them here.

- **Eigenvalue:** The equation (2.1) has solutions only for certain real values α_n of α , and can be ordered as

$$1 > \alpha_0 > \alpha_1 > \alpha_2 > \dots \rightarrow 0, \quad n \rightarrow \infty.$$

- **Double orthogonality:** To each α_n there corresponds only one eigenfunction φ_n . The functions $\{\varphi_n\}_{n=0}^{\infty}$ form dual real orthogonal set both in the interval $(-\infty, \infty)$ and $(-\tau, \tau)$,

$$\int_{-\tau}^{\tau} \varphi_m(t) \varphi_n(t) dt = \alpha_n \delta_{mn}, \quad (2.2)$$

$$\int_{-\infty}^{\infty} \varphi_m(t) \varphi_n(t) dt = \delta_{mn}. \quad (2.3)$$

Here, δ_{mn} is the Delta function, i.e., $\delta_{mn} = 0$ if $m \neq n$ and $\delta_{mn} = 1$ for $m = n$.

- **Completeness:** A bandlimited function y with its Fourier transform support on $[-\sigma, \sigma]$, can be expressed as

$$y(t) = \sum_{n=0}^{\infty} a_n \varphi_n(t), \quad (2.4)$$

where $a_n := \int_{-\infty}^{\infty} y(t) \varphi_n(t) dt$.

- **Fourier transform pair [20]:** The PSWFs φ_n and their Fourier transforms have the following relationships

$$\varphi_n(t) \leftrightarrow (-i)^n \sqrt{\frac{2\pi\tau}{\sigma\lambda_n}} \varphi_n\left(\frac{\tau}{\sigma}\omega\right) p_\sigma(\omega), \quad (2.5)$$

$$\varphi_n(t)p_\tau(t) \leftrightarrow (-i)^n \sqrt{\frac{2\pi\tau}{\sigma}} \varphi_n\left(\frac{\tau}{\sigma}\omega\right) p_\sigma(\omega), \quad (2.6)$$

where p_τ is a characteristic function on $(-\tau, \tau)$, i.e., $p_\tau(t) = 1$ for $t \in (-\tau, \tau)$ and $p_\tau(t) = 0$ for $t \notin (-\tau, \tau)$. p_σ is a characteristic function on $(-\sigma, \sigma)$, i.e., $p_\sigma(\omega) = 1$ for $\omega \in (-\sigma, \sigma)$ and $p_\sigma(\omega) = 0$ for $\omega \notin (-\sigma, \sigma)$.

2.1.2 Discrete Case:

For a discrete $2M + 1$ prolate spheroidal wave sequence $\{\phi_n\}_{n=-M}^M$, which is related to the following trigonometric polynomials (namely digital prolate functions) [4, 20]

$$\phi(t) := \sum_{n=-M}^M \phi_n e^{in\omega_0 t}, \quad (2.7)$$

where $\{\phi_n\}_{n=-M}^M$ satisfied the discrete version of the integral equation Eq. (2.1)

$$\sum_{n=-M}^M \frac{\sin \omega_0 \tau (n-k)}{\pi(n-k)} \phi_k = \lambda_k \phi_n, \quad |n| \leq M, \quad (2.8)$$

where ω_0 is a constant. From the theory of linear equation, Eq. (2.8) has $2M + 1$ eigenvalues $1 > \lambda_0 > \lambda_1 > \lambda_2 > \dots > \lambda_{2M}$. The corresponding eigenvectors $\{\phi_n^k\}$ form an orthonormal set

$$\sum_{n=-M}^M \phi_n^k \phi_n^s = \begin{cases} 1 & k = s, \\ 0 & k \neq s. \end{cases} \quad (2.9)$$

The discrete PSWFs also have the double orthogonality

$$\frac{1}{T} \int_{-\frac{T}{2}}^{\frac{T}{2}} \phi^k(t) \phi^s(t) dt = \sum_{n=-M}^M \phi_n^k \phi_n^s = \begin{cases} 1 & k = s, \\ 0 & k \neq s. \end{cases} \quad (2.10)$$

and

$$\frac{1}{T} \int_{-\frac{T}{2}}^{\frac{T}{2}} \phi^k(t) \phi^s(t) dt = \sum_{n=-M}^M \phi_n^k \phi_n^s \lambda_k = \begin{cases} \lambda_k & k = s, \\ 0 & k \neq s. \end{cases} \quad (2.11)$$

2.2 Maximum Correntropy Criterion

As a popular criterion, the mean square error (MSE) criterion has been widely used in signal processing for decades [23]. This reason is attributed to the low complexity and the analytical tractability of the corresponding algorithms for MSE. For this reason, most previous signal reconstruction methods utilize MSE as the loss function. However, since MSE only consider the second-order statistics, it depends on the Gaussianity assumption of the noise distribution. This makes the MSE based methods sensitive to non-Gaussian noise. Recently, researchers developed the maximum correntropy criterion (MCC) based on information theoretic learning (ITL), which exhibits better robustness to non-Gaussian noise than the MSE [24, 25, 26].

Given two scalar random variables X and Y , the correntropy between X and Y is defined by [27]

$$V(X, Y) := \mathbb{E}[\kappa_\sigma(X - Y)] = \int_{R^2} \kappa_\sigma(x - y)p(x, y)dxdy, \quad (2.12)$$

where \mathbb{E} denotes the expectation, $p(x, y)$ denotes the joint probability density function of X and Y and $\kappa_\sigma(x - y)$ is the Gaussian kernel function given by

$$\kappa_\sigma(x - y) := \frac{1}{\sqrt{2\pi}\sigma} e^{-\frac{(x-y)^2}{2\sigma^2}}. \quad (2.13)$$

Here σ represents the kernel scale. In reality, the joint probability density function $p(x, y)$ is often unknown and only a finite number of samples $\{(x_i, y_i)\}_{i=1}^N$ are available. This leads to the following sample estimator of correntropy

$$\hat{V}(X, Y) := \frac{1}{N} \sum_{i=1}^N \kappa_\sigma(x_i - y_i), \quad (2.14)$$

and the correntropy induced metric (CIM) [15]

$$\text{CIM}(X, Y) := \left\{ \frac{1}{N} \sum_{i=1}^N (\kappa_\sigma(0) - \kappa_\sigma(x_i - y_i)) \right\}^{\frac{1}{2}}. \quad (2.15)$$

Compared to MSE, CIM can handle non-Gaussian noises and give positive performance [15]. This motivates us to utilize the CIM as data fidelity term.

3 Signal Reconstruction

In this section, we first give a brief introduction to the subject of signal reconstruction. Then we present the existing PSWFs based signal reconstruction methods and propose our improved signal reconstruction methods and their corresponding algorithms.

3.1 Background of Signal Reconstruction

The problem of signal reconstruction aims to reconstruct a bandlimited signal $x(t)$ with noise $n(t)$ from some given samples of observed signal $y(t)$ [20]. Specifically, if M samples of the observation signal $y(t)$ are taken at times $\{t_i\}_{i=1}^M$, namely $\mathbf{y} := (y_1, y_2, \dots, y_M)^T \in \mathbb{R}^M$, where $y_i := y(t_i)$, $i = 1, 2, \dots, M$. We would like to reconstruct the bandlimited signal $x(t)$ given by

$$y(t) = x(t) + n(t), \quad t \in \mathbb{R}. \quad (3.1)$$

The classical Shannon sampling theorem shows that the bandlimited signal $x(t)$ can be reconstructed by the samples b_j

$$x(t) = \sum_{n=-\infty}^{+\infty} b_j \frac{\sin \sigma(t - t_j)}{\sigma(t - t_j)}, \quad (3.2)$$

where σ is a constant related to bandwidth. In reality only finite number of samples are available, therefore we consider the finite sum related to sinc-functions $\hat{x}_s(t)$ to approximate $x(t)$,

$$\hat{x}_s(t) := \sum_{j=1}^M b_j \frac{\sin \sigma(t - t_j)}{\sigma(t - t_j)}. \quad (3.3)$$

Denote $\mathbf{b} := (b_1, b_2, \dots, b_M)^T$, $\mathbf{x} := (\hat{x}_{s1}, \hat{x}_{s2}, \dots, \hat{x}_{sM})^T \in \mathbb{R}^M$, where $\hat{x}_{si} = \hat{x}_s(t_i)$, $i = 1, 2, \dots, M$ and

$$(\mathbf{A})_{ij} := \frac{\sin \sigma(t_i - t_j)}{\sigma(t_i - t_j)}, \quad i, j = 1, 2, \dots, M, \quad (3.4)$$

Eq. (3.3) can be written in matrix form as $\mathbf{A}\mathbf{b} = \mathbf{x}$. If \mathbf{b} is given, following Eq. (3.3), then $\hat{x}_s(t)$ is the linear combination of sinc-functions. As an approximation to $x(t)$, the mean-square error (error) between $\hat{x}_s(t)$ and $x(t)$ is given by

$$error := \int_{-\infty}^{+\infty} |x(t) - \hat{x}_s(t)|^2 dt = C \sum_{-\infty < j < 1, j > M} |b_j|^2,$$

where C is a constant.

Giving the observed points $\mathbf{y} = (y_1, y_2, \dots, y_M)^T \in \mathbb{R}^M$ of $y(t)$, they are the vectors \mathbf{x} combining with the white noise, the method of linear least squares is a standard approach to minimize the residual

$$\mathbf{b} = \arg \min_{\mathbf{b} \in \mathbb{R}^M} \|\mathbf{A}\mathbf{b} - \mathbf{y}\|_2^2, \quad (3.5)$$

where $\|\cdot\|_2$ is the ℓ_2 norm. The solution of this problem (3.5) is [30, 31]

$$\mathbf{b} = (\mathbf{A}^T \mathbf{A})^{-1} \mathbf{A}^T \mathbf{y}. \quad (3.6)$$

Utilizing Eq. (3.6), a linear formula $\hat{x}_s(t) = \sum_{j=1}^M b_j \frac{\sin \sigma(t - t_j)}{\sigma(t - t_j)}$ is obtained, where b_j is the i -th component of \mathbf{b} .

3.2 Reconstruction Using PSWFs

The idea for $x(t)$ reconstructed by PSWFs was used in [12] already. However, they just get the reconstruction algorithm using the mean square error (MSE) criterion as the loss function, which will be introduced in the subsection 3.3 in detail. Since the PSWFs are also used in their method, for completeness of the presentation, we list some basic facts for the PSWFs in reconstruction problem.

Using the relationship between sinc-functions and PSWFs [11] $\frac{\sin \sigma(t-t_j)}{\sigma(t-t_j)} = \sum_{m=-\infty}^{+\infty} \phi_m(t)\phi_m(t_j)$, Eq. (3.2) can be expressed by $x(t) = \sum_{j=-\infty}^{+\infty} b_j \sum_{i=-\infty}^{+\infty} \phi_i(t)\phi_i(t_j) = \sum_{j=-\infty}^{+\infty} \left(\sum_{i=-\infty}^{+\infty} b_j \phi_i(t_j) \right) \phi_i(t) = \sum_{j=-\infty}^{+\infty} c_j \phi_j(t)$, where $c_j := \sum_{i=-\infty}^{+\infty} b_j \phi_i(t_j)$. Consider the finite sum of the above series,

$$\hat{x}_\phi(t) := \sum_{j=1}^N c_j \phi_j(t). \quad (3.7)$$

If the coefficients c_j , $j = 1, 2, \dots, N$ of the linear system (3.7) are known, then $\hat{x}_\phi(t)$ can be represented as the linear combination of PSWFs. To find the coefficients c_j , $j = 1, 2, \dots, N$, we first denote the coefficients vector $\mathbf{c} := (c_1, c_2, \dots, c_N)^T$, and solve the following problem

$$\mathbf{c} = \arg \min_{\mathbf{c} \in \mathbb{R}^N} \|\mathbf{D}\mathbf{c} - \mathbf{y}\|_2^2, \quad (3.8)$$

where $\mathbf{D} \in \mathbb{R}^{M \times N}$ and

$$(\mathbf{D})_{ij} := \phi_j(t_i), \quad i = 1, 2, \dots, M, \quad j = 1, 2, \dots, N. \quad (3.9)$$

The solution of this problem is

$$\mathbf{c} = (\mathbf{D}^T \mathbf{D})^{-1} \mathbf{D}^T \mathbf{y}. \quad (3.10)$$

Therefore we obtain a linear formula for \hat{x}_ϕ , $\hat{x}_\phi(t) = \sum_{j=1}^M c_j \phi_j(t)$, where c_j is the i -th component of \mathbf{c} .

Notice that the number of term in Eq. (3.3) and (3.7) are M and N , respectively. The difference comes from the number of the sampling points. The number of samples is M , which means the number of different time also M , i.e., $\{t_i\}_{i=1}^M$. This leads to the Eq. (3.3) has M terms, while Eq. (3.7) can choose different N terms, i.e., the number of PSWFs used can be determined by ourself. Due to the energy concentration property of PSWFs, the number N can be choosn small such that the method preserves most of the energy of the signal.

3.3 Reconstruction Under Regularization and PSWFs

In most of the time the solutions in Eq. (3.6) and Eq. (3.10) may not exist in reality, because the inverse $(\mathbf{A}^T \mathbf{A})^{-1}$ and $(\mathbf{D}^T \mathbf{D})^{-1}$ may not exist. This leads to the ill-posed problems [23, 30, 31]. In these cases, regularization methods are needed to obtain the meaningful solutions. In the following, we will introduce the **Tikhonov regularization based reconstruction algorithm** to overcome the mentioned ill-posed problems.

In [13], Senay *et al.* proposed a method based on the Tikhonov regularization [28, 29] and used the mean square error (MSE) criterion as the cost functions to approximate the target vector \mathbf{c} , i.e.,

$$\mathbf{c} = \arg \min_{\mathbf{c} \in \mathbb{R}^N} \|\mathbf{D}\mathbf{c} - \mathbf{y}\|_2^2 + \lambda \|\mathbf{c}\|_2^2, \quad (3.11)$$

where $\|\cdot\|_2$ is the ℓ_2 norm and λ is the regularization parameter. The explicit solution for this problem (3.11) is

$$\mathbf{c} = (\mathbf{D}^T \mathbf{D} + \lambda \mathbf{I})^{-1} \mathbf{D}^T \mathbf{y}, \quad (3.12)$$

where \mathbf{I} is the identity matrix. Senay *et al.* [13] used the PSWFs \mathbf{D} to obtain the Tikhonov regularization reconstruction (namely, RPSWF).

In the present paper, we compare our method with their RPSWF method. Of course, if the sinc-functions \mathbf{D} is applied to get the Tikhonov regularization reconstruction, we name it RSinc.

3.4 Reconstruction Under Entropy and PSWFs

The mean square error (MSE) criterion in the Eq. (3.11) is known to rely to the problem with Gaussian noise assumption [15, 24]. The vast amount of noise doesn't satisfy this assumption, which leads to the poor reconstruction performance. To overcome this problem, a maximal correntropy based reconstruction method is proposed in this paper. We also noted them as the entropy based methods, such as entropy based PSWFs (EPSWF) and entropy based sinc-functions (ESinc).

We present the signal reconstruction method for entropy based PSWFs (EPSWF) in the following.

Suppose M samples of the observation signal $y(t)$ are taken at times $\{t_i\}_{i=1}^M$. Denote by $\mathbf{y} = (y_1, y_2, \dots, y_M)^T \in \mathbb{R}^M$. Firstly, we use the PSWFs $\{\phi_j(t)\}_{j=1}^N$ to construct the dictionary matrix by defining $(\mathbf{D})_{ij} = \phi_j(t_i)$ for $i = 1, 2, \dots, M$ and $j = 1, 2, \dots, N$. For ease of presentation, denote by \mathbf{d}_i the i -th row of \mathbf{D} .

Secondly, the coefficient vector \mathbf{c} is computed by minimizing

$$\mathbf{c} = \arg \min_{\mathbf{c} \in \mathbb{R}^N} \sum_{i=1}^M (1 - \kappa_\sigma(y_i - \mathbf{d}_i \mathbf{c})) + \lambda \|\mathbf{c}\|_2^2. \quad (3.13)$$

Algorithm 1 Signal reconstruction via EPSWF

Input: The vector $\mathbf{y} \in \mathbb{R}^M$ of samples with $y_i = y(t_i)$, $i = 1, 2, \dots, M$, and the regularization parameter λ .

Output: The recovered signal $\hat{x}_\phi(t)$.

- 1: Construct the matrix $\mathbf{D} \in \mathbb{R}^{M \times N}$ by defining $\mathbf{D}_{ij} = \phi_j(t_i)$ for $i = 1, 2, \dots, M$ and $j = 1, 2, \dots, N$.

Denote by \mathbf{d}_i the i -th row of \mathbf{D} .

- 2: Compute the reconstruction coefficient by solving the following optimization problem

$$\mathbf{c} = \arg \min_{\mathbf{c} \in \mathbb{R}^N} \sum_{i=1}^M (1 - \kappa_\sigma(y_i - \mathbf{d}_i \mathbf{c})) + \lambda \|\mathbf{c}\|_2^2 \quad (3.14)$$

- 3: Calculate the recovered signal $\hat{x}_\phi(t) = \sum_{j=1}^N c_j \phi_j(t)$.

After obtaining the coefficient vector \mathbf{c} , the reconstructed signal is given by

$$\hat{x}_\phi(t) = \sum_{j=1}^N c_j \phi_j(t). \quad (3.15)$$

The complete reconstruction algorithm is summarized in Algorithm 1.

We utilize the half-quadratic theory [32] to design the optimization strategy to solve the problem in Eq. (3.13). According to the convex optimization theory [26, 30], there exists a convex function $\alpha(u)$, $u \in \mathbb{R}$ such that

$$\kappa_\sigma(t) = \sup \left\{ \frac{ut^2}{\sigma^2} - \alpha(u), u \in \mathbb{R}_- \right\}, \quad (3.16)$$

where $u = -\kappa_\sigma(t)$ reaches the supremum. Then there holds

$$-\kappa_\sigma(t) = \inf \left\{ -\frac{ut^2}{\sigma^2} + \alpha(u), u \in \mathbb{R}_- \right\}. \quad (3.17)$$

If we define $w = -\frac{u}{\sigma^2}$ and $\beta(w) = \alpha(u)$, we have

$$-\kappa_\sigma(t) = \inf \left\{ wt^2 + \beta(w), w \in \mathbb{R}_+ \right\}, \quad (3.18)$$

where the infimum is reached at $w = \frac{1}{\sigma^2} \kappa_\sigma(t)$.

Applying the property in Eq.(3.13) and removing constants, we can reformulate the problem in Eq. (3.13) as

$$\min_{\mathbf{c} \in \mathbb{R}^N, \mathbf{w} \in \mathbb{R}_+^M} J(\mathbf{c}, \mathbf{w}) = \sum_{i=1}^M \left(w_i (y_i - \mathbf{d}_i \mathbf{c})^2 + \beta(w_i) \right) + \gamma \|\mathbf{c}\|_2^2, \quad (3.19)$$

where $\mathbf{w} = (w_1, w_2, \dots, w_M)^T \in \mathbb{R}^M$ is a vector composed of auxiliary variables. A local minimizer of problem in Eq. (3.19) can be obtained by alternatively updating \mathbf{c} and \mathbf{w} . Specifically, while fixing the coefficient vector \mathbf{c} , the auxiliary vector \mathbf{w} can be updated by setting

$w_i^{(t+1)} = \frac{1}{\sigma^2} \kappa_\sigma(y_i - \mathbf{d}_i \mathbf{c}^{(t)})$, $i = 1, 2, \dots, M$ according to the analysis above. Here t is the number of iterations. While fixing \mathbf{w} , the problem in Eq. (3.19) is equivalent to

$$\mathbf{c}^{(t+1)} = \arg \min_{\mathbf{c} \in \mathbb{R}^n} \left\| \sqrt{\text{diag}(\mathbf{w}^{(t+1)})} \mathbf{y} - \sqrt{\text{diag}(\mathbf{w}^{(t+1)})} \mathbf{D} \mathbf{c} \right\|_2^2 + \lambda \|\mathbf{x}\|_2^2. \quad (3.20)$$

where $\text{diag}(\mathbf{w}^{(t+1)})$ denotes a square diagonal matrix with the elements of $\mathbf{w}^{(t+1)}$ on the main diagonal.

The optimization problem in Eq. (3.24) has a close form solution, which can be explicitly expressed as

$$\mathbf{c}^{(t+1)} = (\mathbf{D}^T \text{diag}(\mathbf{w}^{(t+1)}) \mathbf{D} + \lambda \mathbf{I})^{-1} \mathbf{D}^T \text{diag}(\mathbf{w}^{(t+1)}) \mathbf{y}. \quad (3.21)$$

As for the kernel size σ , it is determined empirically [16] and set as

$$\sigma = \left(\frac{1}{2M} \|\mathbf{y} - \mathbf{D} \mathbf{c}\|_2^2 \right)^{\frac{1}{2}}. \quad (3.22)$$

Algorithm 2 summarizes the complete procedure for solving the problem in Eq. (3.13). In light of the half-quadratic theory [32], the sequence $\{J(\mathbf{c}^{(t)}, \mathbf{w}^{(t)})\}_{t=1}^{\infty}$ always converges.

Algorithm 2 Solving the optimization problem in Eq. (3.13)

Input: \mathbf{y} , \mathbf{D} , λ .

Output: \mathbf{c} .

Repeat until convergence:

1: Update the auxiliary variables $\{w_i\}_{i=1}^{i=M}$

$$w_i^{(t+1)} = \frac{1}{\sigma^2} \kappa_\sigma(y_i - \mathbf{d}_i \mathbf{c}^{(t)}), \quad i = 1, 2, \dots, M. \quad (3.23)$$

2: Update the coefficient vector \mathbf{c}

$$\mathbf{c}^{(t+1)} = \arg \min_{\mathbf{c} \in \mathbb{R}^N} \left\| \sqrt{\text{diag}(\mathbf{w}^{(t+1)})} \mathbf{y} - \sqrt{\text{diag}(\mathbf{w}^{(t+1)})} \mathbf{D} \mathbf{c} \right\|_2^2 + \lambda \|\mathbf{x}\|_2^2. \quad (3.24)$$

4 Experiments

In this section, we present the the performance of the proposed methods by applying them to a signal $x(t)$. The signal $x(t)$ is a combination of three sinusoids original signals embedded in noise, i.e.,

$$x(t) = \sin(50t + 0.1) + \sin(30t + 0.8) + \sin(40t + 0.5), \quad 0 \leq t \leq 1. \quad (4.1)$$

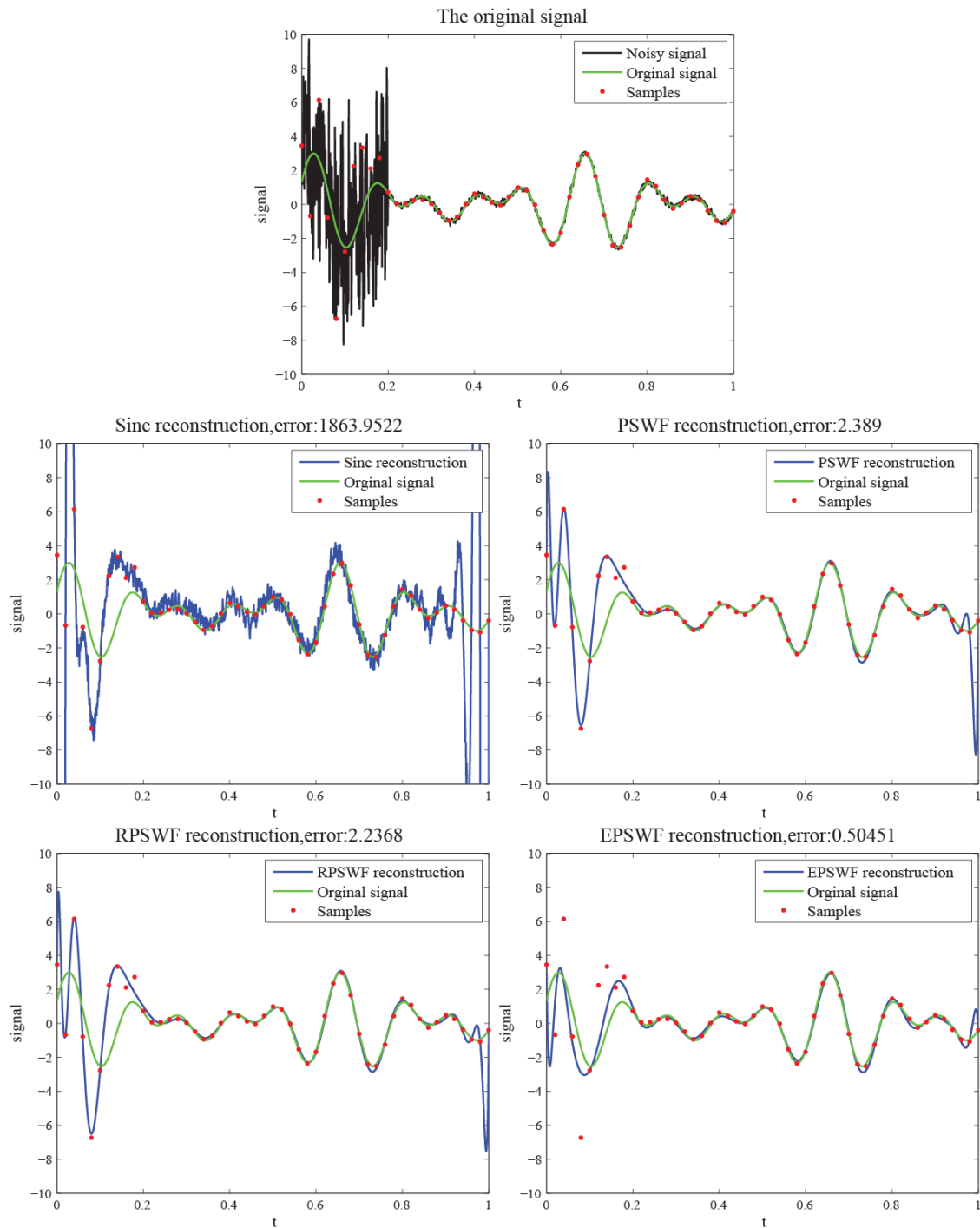


Figure 1: Results for uniformly sampled signal reconstruction and error. The first image shows the original signal with noise and the samples. The following 4 images show the reconstructed signals in blue lines with different methods. The Sinc-functions method with reconstructed error 1863.9522; the PSWF method with reconstructed error 2.3890; the RPSWF method with reconstructed error 2.2368; the EPSWF method with reconstructed error 0.5045.

In Fig. 1 and 2, the green line is the original signal $x(t)$ for $0 \leq t \leq 1$.

The experiments include two parts, the first one is about the signal with a large quantity of noise in $0 \leq t \leq 0.2$, which is shown in Fig. 1 the black line. While the second experiment add a small quantity of noise in $0 \leq t \leq 0.2$, which is shown in Fig. 2 the black line.

In the first experiment, we uniformly sample some sample points, which is shown in red points in Fig. 1. Since the large noise added in the signal, some of samples in $0 \leq t \leq 0.2$ are far away from the original signal. The blue lines in Fig. 1 shows the reconstructed results for different methods. In more specific terms, the methods include Sinc, PSWF, RPSWF and EPSWF. The reconstructed error are also shown in these pictures. From the Fig. 1, we can obtain the following conclusions:

- The PSWFs based method is greater than the sinc-functions based method.
- The Tikhonov regularization based reconstruction method (RPSWF) is better than the non-regularization methods (PSWF and sinc-functions).
- The maximal correntropy based Reconstruction method (EPSWF) is the best method among all of the methods.

However, we can find the the reconstruction error for RPSWF 2.2368 is not much to improve than that of PSWF method 2.3890. While, the reconstruction error for EPSWF 0.5045 is much smaller than 2.2368. This results verify the superiority of EPSWF for signal with large noise.

In the second experiment, we non-uniformly sample some sample points, which is shown in red points in Fig. 2. The samples in $0 \leq t \leq 0.2$ are intensive and the samples in $0.2 \leq t \leq 1$ are sparse. The blue lines in Fig. 2 shows the reconstructed results for different methods. Since we have known that the regularization based and maximal correntropy based reconstruction methods have good performance, we only compare these methods in this experiments. In more specific terms, the methods include RSinc, PSinc, RPSWF and EPSWF. The reconstructed error are shown in pictures. From the Fig. 2, we can obtain the following conclusions:

- The RPSWF based method is significantly better than the RSinc based method and the EPSWF based method is far better than the ESinc based method, i.e., the PSWFs based method is better than sinc-functions based method.
- The EPSWF based method is far better than the RPSWF based method and ESinc based method is far better than the RSinc based method, i.e., the maximal correntropy based reconstruction methods is better than the regularization based reconstruction methods.

5 Conclusions

In this paper, we proposed a novel robust signal reconstruction method based on the prolate spherical wave functions (PSWFs) and maximum correntropy criterion (MCC). The PSWFs have been proven to have good performance in signals representation. But the existed PSWFs method only consider the MSE criterion method, which has good performance for noise obey

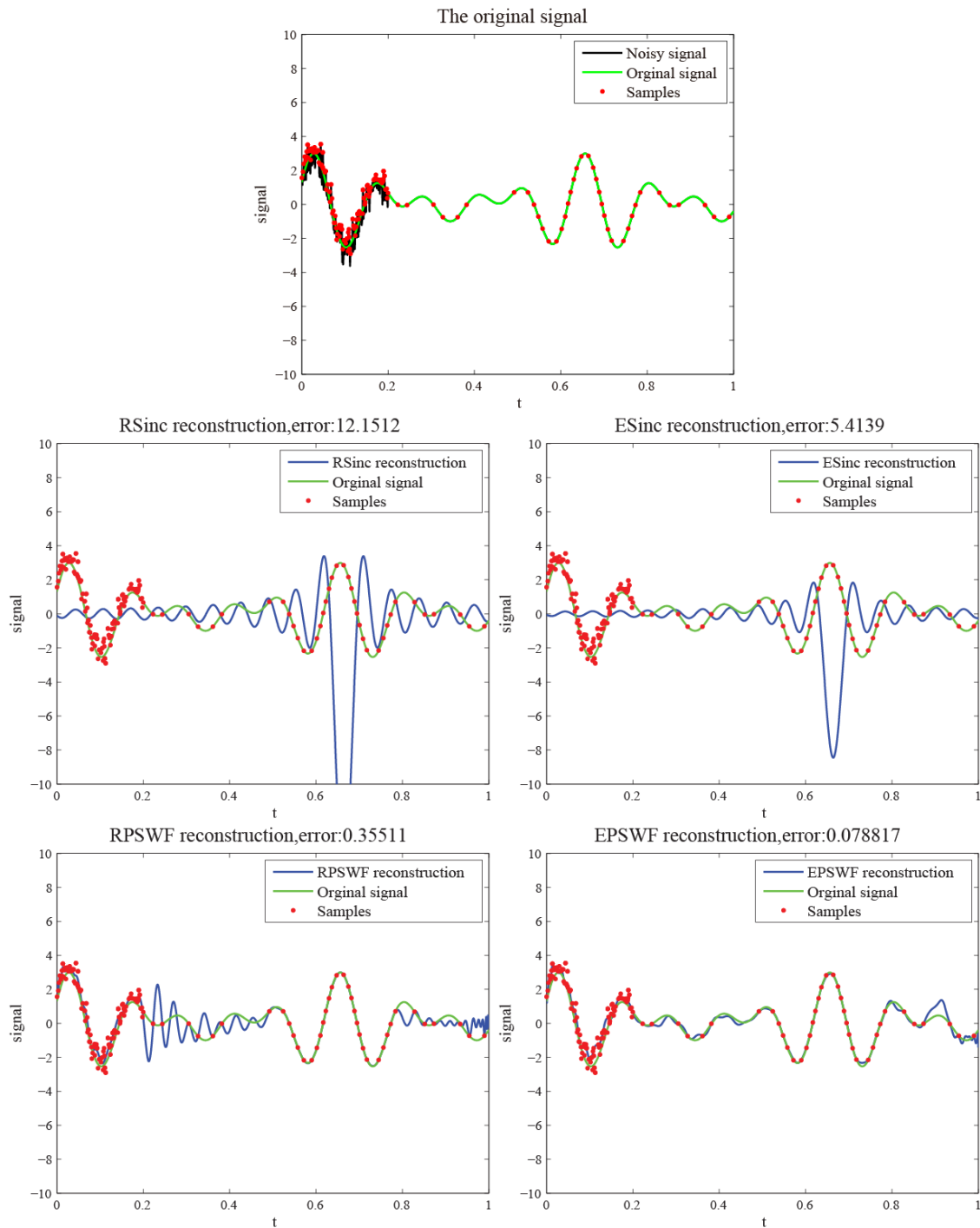


Figure 2: Results for nonuniformly sampled signal reconstruction and error. The first image shows the original signal with noise and the samples. The following 4 images show the reconstructed signals in blue lines with different methods. The RSinc method with reconstructed error 12.1515; the ESinc method with reconstructed error 5.4139; the RPSWF method with reconstructed error 0.3551; the EPSWF method with reconstructed error 0.0788.

the Gaussian distribution. For the impulsive noise and outliers, the MSE based method leads to

large reconstruction error. For these reasons, we proposed the MCC based PSWFs reconstruction method (EPSWF). The experimental results on synthetic signals show that the EPSWF can obviously improve the performance in signal reconstruction.

References

- [1] A. Jeffrey and D. L. Joseph, *Duration and bandwidth limiting: Prolate Functions, Sampling, and Applications*. Springer Science and Business Media, 2011.
- [2] D. Slepian and H. Pollak, "Prolate spheroidal wave functions, fourier analysis, and uncertainty-I," *Bell System Technical Journal*, 40(1961), 43-64.
- [3] D. Slepian, "Prolate spheroidal wave functions, fourier analysis and uncertainty-IV: Extensions to many dimensions; generalized prolate spheroidal functions," *Bell System Technical Journal*, 43(6)(1964), 3009-3057.
- [4] D. Slepian, "Prolate Spheroidal Wave Functions, Fourier Analysis, and Uncertainty -V: The Discrete Case," *Bell System Technical Journal*, 57(5)(1978), 1371-1430.
- [5] A. Karoui, "Uncertainty Principles, Prolate Spheroidal Wave Functions, and Applications," *Applied and Computational Harmonic Analysis*, 16(3)(2004), 208–230.
- [6] I. C. Moore and M. Cada, "Prolate spheroidal wave functions, an introduction to the Slepian series and its properties," *Applied and Computational Harmonic Analysis*, 16(2004), 208–230.
- [7] C. E. Shannon, "Communication in the presence of noise," *Proc. Institute of Radio Engineers*, 37(1)(1949), 10–21.
- [8] G. Walter and X. Shen, "Sampling with prolate spheroidal wave functions," *Sampling Theory in Signal Image Processing*, 2(2003), 25–52.
- [9] K. Khare and N. George, "Sampling theory approach to prolate spheroidal wave functions," *Journal of Physics: Mathematical and General*, (2003).
- [10] T. Moumni and A. I. Zayed, "A generalization of the prolate spheroidal wave functions with applications to sampling," *Integral Transforms and Special Functions*, (2014), 1–15.
- [11] D. Cheng and K. I. Kou, "Sampling by quaternion reproducing kernel Hilbert space embedding," *Preprint*.
- [12] S. Senay, L. F. Chaparro, and L. Durak, "Reconstruction of nonuniformly sampled time-limited signals using prolate spheroidal wave functions," *Signal Processing*, 89 (2009), 2585–2595.

- [13] S. Senay, J. Oh, and L. F. Chaparro, “Regularized signal reconstruction for level-crossing sampling using Slepian functions,” *Signal Processing*, 92(2012), 1157–1165.
- [14] D. Pham and S. Venkatesh, “Improved image recovery from compressed data contaminated with impulsive noise,” *IEEE Trans. Image Process.*, 21(1)(2012), 397–405.
- [15] W. Liu and P. P. Pokharel and J. C. Principe, “Correntropy: properties and applications in non-gaussian signal processing,” *IEEE Trans. Signal Process.*, 55(11)(2007), 5286-5298.
- [16] J. C. Principe, “Information Theoretic Learning: Renyi’s Entropy and Kernel Perspectives,” *New York, NY, USA: Springer-Verlag*, 2010.
- [17] D. Slepian, “Some comments on Fourier analysis, uncertainty and modeling,” *SIAM Rev.*, 25 (3) (1983) 379–93.
- [18] H. J. Landau and H. O. Pollak, “Prolate Spheroidal Wave Functions, Fourier Analysis and Uncertainty - II,” *Bell System Technical Journal*, 40(1)(1961), 65–84.
- [19] H. J. Landau and H. O. Pollak, “Prolate spheroidal wave functions, Fourier analysis and uncertaintyC III: The dimension of space of essentially time-and bandlimited signals,” *Bell System Technical Journal*, 41(4)(1962), 1295–1336.
- [20] A. Papoulis, “Signal analysis,” *McGraw-Hill Press*, 1977.
- [21] J. Kondo, “Integral equations,” *Clarendon Press/Oxford University Press*, 1992.
- [22] Z. S. Michael, “The classical theory of integral equations a concise treatment,” *New York: Birkhäuser Press*, 2012.
- [23] V. Chandrasekaran, B. Recht, P. A. Parrilo, and A. S. Willsky, “The convex geometry of linear inverse problems,” *Found. Comput. Math.*, 12(2012), 805–849.
- [24] R. He, W. Zheng, and B. Hu, “Maximum correntropy criterion for robust face recognition,” *IEEE Trans. Pattern Anal. Mach. Intell.*, 33(8)(2011), 1561–1576.
- [25] D. Erdogmus and J. C. Principe, “An error-entropy minimization algorithm for supervised training of nonlinear adaptive systems,” *IEEE Trans. Signal Process.*, 50(7)(2002), 1780–1786.
- [26] Y. Wang, Y. Y. Tang, and L. Li, “Robust Face Recognition via Minimum Error Entropy based Atomic Representation,” *IEEE Trans. Image Process.*, 24(12)(2015), 5868–5878.
- [27] A. Rnyi, *Probability Theory*. Amsterdam, The Netherlands: Elsevier, 1970.
- [28] S. Orintara, W. C. Karl, D. A. Castanon, and T. Q. Nguyen, “A method for choosing the regularization parameter in generalized Tikhonov regularized linear inverse problems,” *International Conference on Image Processing*, 1(2000), 93–96.

- [29] A. N. Tikhonov, "Solution of incorrectly formulated problems and the regularization method," *Soviet Mathematics–Doklady*, 4(1963), 1035–1038.
- [30] R. Rockfellar, "Convex analysis," *Princeton Press*, 1970.
- [31] P. C. Hansen, "Rank-deficient and discrete ill-posed problems: numerical aspects of linear inversion," *SIAM, Mathematical Modeling and Computation*, (1998).
- [32] M. Nikolova and M. K. Ng, "Analysis of half-quadratic minimization methods for signal and image recovery," *SIAM J. Sci. Comput.*, 27(3)(2005), 937-966.